IEEE Access
Multidisciplinary | Rapid Review | Open Access Journal

Received August 26, 2019, accepted September 12, 2019, date of publication September 20, 2019, date of current version October 17, 2019.

Digital Object Identifier 10.1109/ACCESS.2019.2942632

TH-NRDCSK: A Non-Coherent Time Hopping Chaotic System for Anti-Jamming Communications

JUNGMIN KIM [1], (Member, IEEE), BINH VAN NGUYEN [2], HYOYOUNG JUNG [1], (Student Member, IEEE), AND KISEON KIM [1], (Senior Member, IEEE)

[1]Gwangju Institute of Science and Technology, Gwangju 500-712, South Korea
[2]Institute of Research and Development, Duy Tan University, Da Nang 550000, Vietnam

Corresponding author: Kiseon Kim (kskim@gist.ac.kr)

This work was supported by the Electronic Warfare Research Center, Gwangju Institute of Science and Technology (GIST), originally funded by Defense Acquisition Program Administration (DAPA) and Agency for Defense Development (ADD).

ABSTRACT Time hopping spread spectrum (THSS) system and chaotic system have been studied as candidates of the anti-jamming (AJ) systems with substantial advantages. However, THSS systems suffer from the strict synchronization prerequisite. In order to overcome the shortcomings of the THSS system and utilize the profits of the non-coherent chaotic system, we first propose a novel TH-NRDCSK system to enhance the bit error rate (BER) performance of the conventional non-coherent THSS system and relieve the strict synchronization issue of coherent THSS systems. Then, we analyze the performance of the proposed system under additive white Gaussian noise (AWGN) channel and jamming environment. Finally, we implement the simulation to demonstrate the consistency of the analysis and the simulation results and to disclose the effects of the system parameters on system's AJ performance. Moreover, the performance of the proposed system is compared to that of conventional counterparts to look at the benefits of integrating chaotic and THSS systems. The simulation results show that the proposed system significantly outperforms conventional counterparts in a practical environment.

INDEX TERMS Time hopping - noise reduction differential chaos shift keying (TH-NRDCSK) system, time hopping (TH) system, noise reduction - differential chaos shift keying (NR-DCSK) system, anti-jamming (AJ) system, non-coherent system.

GLOSSARY

AJ	Anti-Jamming
AWGN	Additive White Gaussian Noise
BBNJ	Broad Band Noise Jamming
BER	Bit Error Rate
CSK	Chaotic Shift Keying
DCSK	Differential Chaotic Shift Keying
EA	Electronic Attack
EP	Electronic Protection
ES	Electronic Support
EW	Electronic Warfare
LPI	Low Probability of Intercept
MTJ	Multi Tone Jamming
NR-DCSK	Noise Reduction Differential Chaotic Shift Keying
PBNJ	Partial Band Noise Jamming
SJ	Sweep Jamming
STJ	Single Tone Jamming
TH	Time Hopping
TH-NRDCSK	Time Hopping Noise Reduction Differential Chaotic Shift Keying
THSS	Time Hopping Spread Spectrum
TJ	Tone Jamming
UWB	Ultra Wide Band

The associate editor coordinating the review of this manuscript and approving it for publication was Yongpeng Wu.

I. INTRODUCTION

Electronic warfare (EW) includes attacking an enemy (electronic attack, EA), protecting against enemy attacks (electronic protection, EP), and detecting/intercepting

electromagnetic energy (electronic support, ES) [1]. In an EW environment, military operations are executed along with increasingly complex demands for electromagnetic spectrum. Among many military operations, EP has been a crucially important issue due to the development of attacking technologies. EP basically focuses on eliminating, reducing, or mitigating the implication of the desired or undesired signals. Anti-jamming (AJ) is one of EP technologies in the physical layer of wireless communication system and has been investigated. In other words, AJ technology is of utmost concern to realize reliable and covert communication [2].

Time hopping spread spectrum (THSS) technology is considered to be one of the most efficient AJ technologies with its powerful characteristics, such as ultra-wide band (UWB) and low transmit power density and robustness to jamming signals [3]–[6]. In addition, this system inherently offers resilience to multipath fading and multiple access capabilities. These advantages are due the fact that the THSS system obtains UWB by transmitting information bits with extremely narrow pulses (called monocycle). Despite these advantages, THSS systems require strict synchronization, which is why their applications are limited in reality. To address this issue, non-coherent THSS systems have been proposed in [7], yet its bit error rate (BER) performance are much worse than that of the coherent ones.

On the other hand, chaotic systems and their related applications for covert communication have widely been studied over the past several decades [8]–[17]. Chaotic systems also have significant advantages in AJ and LPI applications by utilizing non-linear signals [18]. Chaotic systems can be classified as coherent or non-coherent ones [19]. Chaotic shift keying (CSK) is a fundamental coherent system. CSK system is complicated in practice due to the prerequisite of chaotic synchronization at the receiver. Another system is the differential chaotic shift keying (DCSK) system, which is a basic and simple non-coherent chaotic system, that does not require chaotic synchronization as well as channel state information for decoding. Even though the DCSK system has inherently worse performance than the CSK counterpart, it has been preferred in practical wireless communication due to its simplicity. In order to improve the performance of the DCSK system, several advanced alternatives have recently been proposed, i.e. high efficiency-DCSK [20], improved-DCSK [21], short reference-DCSK [22], reference modulated-DCSK [23], noise reduction-DCSK [24], among which the NR-DCSK scheme seems to be the most efficient. The NR-DCSK system utilizes repetition of chaotic samples so that the repeated samples are averaged at the receiver to reduce the effect of noise.

To enjoy advantages of both the THSS system and the NR-DCSK system with less complexity for AJ communication, we propose a novel TH-NRDCSK system, which is a combination of the THSS system and the NR-DCSK system. The integration of these two systems will allow us to utilize the advantages of both systems. In order to verify the AJ performance of the proposed system, we analyze the system performance under an additive white Gaussian noise (AWGN) channel and a broad band noise jamming (BBNJ) environment. We derive a closed form expression of the system BER. Moreover, we simulate the proposed TH-NRDCSK system performance under several simulation setups to illustrate the effect of system parameters, i.e. the number of repeated bits for one bit N_s, the number of time hopping slot for one repeated bit N_h, the number of repeating one chaotic sample P, and the length of subslot β. The AJ performances of the TH-NRDCSK system and other conventional counterparts are also compared. Eventually, we observe several insights about the effects of system parameters through the analytic and simulation results and show that the TH-NRDCSK system is more robust than some of the other aforementioned systems. We also show that the proposed system can outperform coherent THSS and chaotic systems if synchronization errors occur.

The remainder of this paper is organized as follows. The conventional THSS system and NR-DCSK system are briefly introduced and the proposed TH-NRDCSK system is proposed in Section II. The BBNJ, partial band noise jamming (PBNJ), tone jamming (TJ), sweep jamming (SJ) models are depicted in section III. The BER expression for the proposed system under AWGN and BBNJ environment is derived in section IV. The simulation results of the proposed TH-NRDCSK system under several conditions, and the conclusions are presented in Section V and VI, respectively.

II. SYSTEM MODELS

In this section, we briefly introduce the conventional THSS system and NR-DCSK system, and thoroughly elaborate on the TH-NRDCSK system. Table 1 shown at the top of next page describes the system parameters and whether they are used for respective systems.

A. THSS SYSTEM

Time hopping spread spectrum (THSS) is a promising technology due to its advantageous features. A THSS system uses a very short time pulse, referred to as monocycles, for UWB and low transmitted power spectral density. The process of generating transmitted signal is as follows. First, the information bits are repeated several times. Secondly, each repeated bits has one very short time pulse. Specifically, the i-th short time pulse is allocated in the c_i-th time hopping slot to make a mask signal. Finally, the transmit signal is created by multiplying information bit with the mask signal. The transmitted signal $s_{tr}^{(j)}\left(u, t^{(j)}\right)$ with antipodal modulation can be expressed as [4]

$$s_{tr}^{(j)}\left(u, t^{(j)}\right) = \sum_{i=-\infty}^{\infty} d_i^{(j)}(u) w_{tr}\left(t^{(j)} - iT_f - c_i^{(j)}(u)T_c\right), \quad (1)$$

where $t^{(j)}$ is the j-th transmitter clock time, $w_{tr}(t)$ is the transmitted monocycle waveform. T_f, c_i, T_c, and d_i represents the pulse train spacing (frame) time, TH sequence, chip time, and modulation repeated bits, respectively. Then, the receiver

TABLE 1. System parameters.

Parameters	Meaning	THSS	NR-DCSK	TH-NRDCSK
l	The index of bits	o		
i	The index of repeated bits	o	x	o
c_i	i-th time hopping code	o	x	o
k	The index of chaotic samples	x	o	o
β	The length of sequence in one subslot	x	o	o
P	The number of repeating one chaotic sample	x	o	o
f_s	Sampling frequency	o		
T_c	Chip time, one time hopping slot interval	o		
N_h	The number of time hopping slot in one repeated bit	o	x	o
N_s	The number of repeating one bit	o	x	o
N_t	The period of time hopping code	o	x	o
E_b/N_0	Energy per bit to noise power spectral density ratio	o		
SJR	Signal to jamming power ratio	o		

receives the signal, which has been distorted by the noise and interference, and correlates the received signal with mask signal coherently. The original bits are restored by summing the correlated results and comparing the results with a threshold.

The coherent THSS system utilizes the subnanosecond pulses at the transmitter, and correlates the received signal with a mask signal at the receiver. This causes time synchronization issues on the coherent THSS system. Consequently, non-coherent THSS systems were proposed to address the time synchronization problem [7]. However, the non-coherent THSS systems are shown to have poor performance.

B. NR-DCSK SYSTEM

Chaotic communication has also been considered to be a powerful method in AJ communication applications. The NR-DCSK system repeats each chaotic sample P times at the transmitter side so that the received signal can be averaged at the receiver side to reduce the noise effect. The specific process of the NR-DCSK system is as follows. First, a chaotic sequence of length β/P is generated by the logistic map which provides simplicity and good performance. The logistic map is expressed as [25]

$$x_{k+1} = 1 - 2x_k^2, \tag{2}$$

where the expectation of x_k, $E[x_k] = 0$, and the variance of x_k, $V[x_k] = 1$ for normalized x_k. Secondly, β/P chaotic samples are repeated P times to make the reference sequence of β length. Then, the information sequence is created by multiplying the l-th bit and the reference sequence. The sequence of the transmitted signal is made by concatenating the reference sequence and the information sequence. As a result, the transmitted signal of the l-th bit, b_l, can be

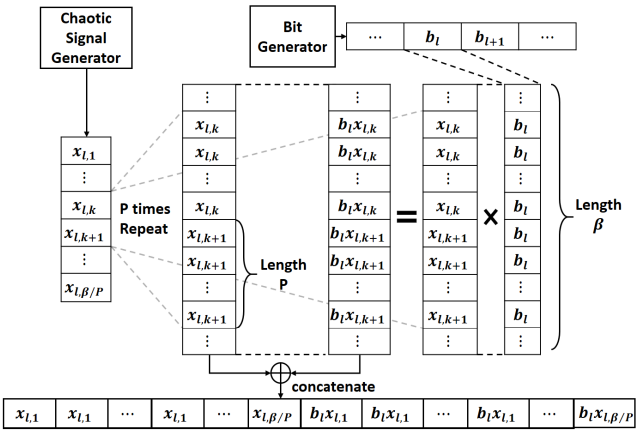

FIGURE 1. Bit generation process of the NR-DCSK system.

represented by [24]

$$s_{l,k} = \begin{cases} x_{i,\lceil \frac{k}{P} \rceil}, & 0 < k \le \beta, \\ b_l x_{i,\lceil \frac{k}{P} \rceil}, & \beta < k \le 2\beta. \end{cases} \tag{3}$$

The bit generation process of the NR-DCSK system is illustrated in Fig. 1. At the receiver, the received signal is averaged using a block average filter of size P and correlated with its time delayed version by a factor of β/P. The transmitted bit is then estimated by summing the correlation results and passing the outcome through a threshold detector.

C. TH-NRDCSK SYSTEM

The TH-NRDSCK system is a combination of THSS system and the NR-DCSK system. The system block diagram is illustrated in Fig. 2. Instead of using conventional THSS pulses, i.e. rectangle monocycle, Gaussian pulse, Gaussian

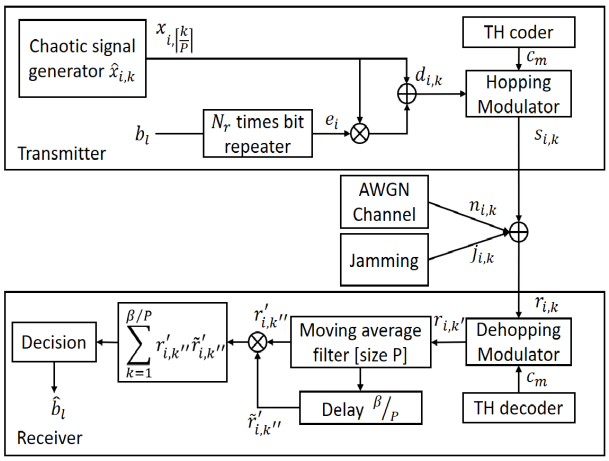

FIGURE 2. System architecture of the TH-NRDCSK system.

monocycle, and Gaussian doublet, NR-DCSK signal is generated at the chaotic signal generator. In addition, the received NR-DCSK signal is averaged by moving average filter at the receiver side.

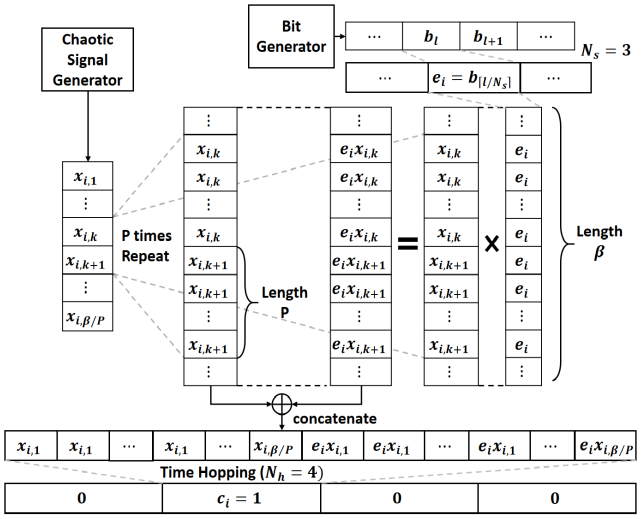

FIGURE 3. Bit generation process of the TH-NRDCSK system.

Fig. 3 presents how the TH-NRDCSK transmitted signal $s_{i,k}$ is generated. Each transmitted bit, b_l is repeated N_s times in its respective subframe. These repeated bits, e_i, can be written as $b_{\lceil \frac{i}{N_r} \rceil}$. Then each repeated bit, e_i in the subframe is expanded into N_h time hopping slots. Only one of these slots contains useful information for each e_i. This specific slot is selected through a predetermined TH code, c_i, which corresponds to a specific i value for each e_i. This slot is decomposed into two subslots of length β, where the first subslot has a reference sequence of $x_{i,k}$ repeated P times for each k until $k = \beta/P$, and the second subslot has an information sequence equal to the reference sequence multiplied by e_i. $x_{i,k}$ is a chaotic sequence generated by a logistic chaotic map.

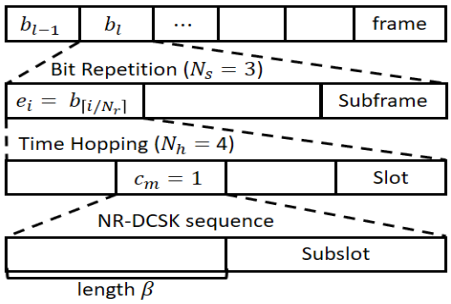

FIGURE 4. Bit structure of the TH-NRDCSK system.

In addition, $x_{i,\lceil \frac{k}{P} \rceil}$ represents a $x_{i,k}$ element repeated P times in a NR-DCSK subslot. Note that P is the number of times that one chaotic sample is repeated so that P is divisor of β, and the length of chaotic sequences required to complete a single subframe is β/P. A graphical illustration of the bit structure of the TH-NRDCSK system is given in the Fig. 4. Mathematically, $s_{i,k}$ can be expressed as

$$s_{i,k} = \begin{cases} x_{i,\lceil \frac{k}{P} \rceil}, & c_i T_c f_s < k \leq c_i T_c f_s + \beta, \\ e_i x_{i,\lceil \frac{k}{P} \rceil - \beta}, & c_i T_c f_s + \beta < k \leq c_i T_c f_s + 2\beta. \end{cases} \tag{4}$$

The signal $s_{i,k}$ is transmitted through a AWGN channel and corrupted by jamming signal. The received $r_{i,k}$ at the destination can be expressed as

$$r_{i,k} = s_{i,k} + n_{i,k} + j_{i,k}, \tag{5}$$

where $n_{i,k}$ is the AWGN and $j_{i,k}$ is the jamming signal. The AWGN channel is considered for analysis simplicity. The receiver gets $r_{i,k'}$ by using the same TH code, c_i, to select one time hopping slot which contains valid information signals. After that, the receiver creates $r'_{i,k''}$ by passing $r_{i,k'}$ through the moving average filter of window size P. $r'_{i,k''}$ is given by

$$\begin{aligned} r'_{i,k''} &= \sum_{m=1}^{\beta/P} \frac{1}{P} \sum_{k'=(m-1)P+1}^{mP} r_{i,k'} \\ &= s_i + \frac{1}{P} \sum_{k'=(m-1)P+1}^{mP} n_{i,k'} + \frac{1}{P} \sum_{k'=(m-1)P+1}^{mP} j_{i,k'}. \end{aligned} \tag{6}$$

This operation makes the sequence of length β/P and reduces the noise effect. The signal $r'_{i,k''}$ is correlated with its time delay version $r'_{i,k''+\beta/P}$. Then, the reconstructed repeated bits $\hat{e}_i$ are recovered by comparing the correlation output with a threshold. By doing so, the original bit $\hat{b}_l$ is recovered by applying the hard decision method that uses N_s repeated bits. The decision variable of the repeated bits e_i at the correlation output, D_i, can be written as

$$\begin{aligned} D_i = \sum_{k=1}^{\beta/P} &\left(x_{i,\lceil \frac{k}{P} \rceil} + \bar{n}_{i,k'} + \bar{j}_{i,k'} \right) \\ &\cdot \left(e_i x_{i,\lceil \frac{k}{P} \rceil} + \bar{n}_{i,k'+\beta} + \bar{j}_{i,k'+\beta} \right), \end{aligned} \tag{7}$$

where $\bar{n}_{i,k'}$ and $\bar{j}_{i,k'}$ are $\frac{1}{P}\sum_{k'=(k-1)P+1}^{kP} n_{i,k'}$ and $\frac{1}{P}\sum_{k'=(k-1)P+1}^{kP} j_{i,k'}$ which are the noise and jamming signal after passing through the moving average filter. In addition, $\bar{n}_{i,k'+\beta}$ and $\bar{j}_{i,k'+\beta}$ denote the β/P delayed version of $\bar{n}_{i,k'}$ and $\bar{j}_{i,k'}$. Then, the decision variable may be further expanded as

$$D_i = \sum_{k=1}^{\beta/P} \Bigg[\underbrace{e_i\left(x_{i,\lceil \frac{k}{P} \rceil}\right)^2}_{U} + \underbrace{x_{i,\lceil \frac{k}{P} \rceil}\bar{n}_{i,k'}}_{N_1} + \underbrace{e_i x_{i,\lceil \frac{k}{P} \rceil}\bar{n}_{i,k'}}_{N_2} + \underbrace{\bar{n}_{i,k'}\bar{j}_{i,k'+\beta}}_{N_3} + \underbrace{\bar{j}_{i,k'}\bar{n}_{i,k'+\beta}}_{N_4} + \underbrace{\bar{n}_{i,k'}\bar{n}_{i,k'+\beta}}_{N_5} + \underbrace{x_{i,\lceil \frac{k}{P} \rceil}\bar{j}_{i,k'+\beta}}_{I_1} + \underbrace{e_i x_{i,\lceil \frac{k}{P} \rceil}\bar{j}_{i,k'}}_{I_2} + \underbrace{\bar{j}_{i,k'}\bar{j}_{i,k'+\beta}}_{I_3} \Bigg], \tag{8}$$

where U and N_1, N_2, N_3, N_4 and N_5 represent the data and noise components, and I_1, I_2, and I_3 represent the interference components.

III. JAMMING MODELS

A. BROAD BAND NOISE JAMMING (BBNJ) [26]

Broad band noise jamming (BBNJ) is generated by allocating jamming energy over the whole frequency bandwidth with equal amounts of power. The frequency bandwidth is assumed to be the bandwidth used by the target signal. In other words, BBNJ increases the noise intensity at the receiver evenly, which makes legitimate communicate more difficult to operate properly. The BBNJ is commonly regarded as a zero-mean Gaussian random variable with power P_j. Then, the power spectral density of BBNJ is $P_j/2W$, where W is the bandwidth of transmitted signal.

B. PARTIAL BAND NOISE JAMMING (PBNJ) [27]

Partial band noise jamming (PBNJ) signal disrupts a portion of the bandwidth of the transmitted signal with equally concentrated power. Since the jammer uses less bandwidth and more power for the given bandwidth, PBNJ is considered to be more effective than BBNJ. Once the jammer concentrates its power to affect a valid fraction of the transmitted signal, the jammed signal will be incorrectly decoded with a high probability. The power of PBNJ signal will be concentrated to a bandwidth ρW, where ρ is the ratio of frequency domain occupancy ($0 < \rho \leq 1$). The PBNJ signal is a band-limited Gaussian noise with a flat power spectral density over the jammed bandwidth, i.e., the power spectral density in the jammed band is $P_j/2\rho W$.

C. TONE JAMMING (TJ) [28]

Tone Jamming (TJ) is also considered as an efficient jamming method due to the fact that the jamming signal attacks one or more frequencies of the target signals' spectrum strategically. TJ is categorized as single tone jamming (STJ) or multi tone jamming (MTJ). STJ includes only one sinusoidal signal having the concentrated power, while MTJ includes several sinusoidal signals which have equally divided power. Mathematically, the TJ can be expressed as

$$J_{TJ}(t) = \sum_{m=1}^{M} \sqrt{\frac{2P_j}{M}} \sin\left(2\pi f_m t + \theta_m\right), \tag{9}$$

where M, P_j, f_m, and θ_m are the number of jamming tones, total jamming power, the frequency, and the phase of the m-th jamming signal, respectively.

D. SWEEP JAMMING (SJ) [29]

Sweep Jamming (SJ) signal changes its frequency periodically over a certain frequency band and time. In this way, SJ is considered to be efficient by utilizing the advantages of both TJ and PBNJ. The frequency f_{SJ} of the SJ signal can be expressed by the following equation

$$f_{SJ}(t) = f_l + (f_u - f_l)\, t \big/ T_{SJ}, \tag{10}$$

where f_l, f_u, and T_{SJ} are lower bound of the jamming frequency, upper bound of the jamming frequency, and the period of sweep, respectively. Then, a sweep jamming signal can be expressed as

$$J_{SJ}(t) = \sqrt{2P_j}\cos\left(f_l t + \frac{f_u - f_l}{2T_{SJ}}t^2 + \theta_{SJ}\right), \tag{11}$$

where P_j is the power of the jamming signal and θ_{SJ} is the phase delay of the jamming signal.

IV. PERFORMANCE ANALYSIS

In this section, we derive the theoretical performance of the proposed TH-NRDCSK system under the AWGN channel and BBNJ jamming environment. For i-th repeated bit e_i, the repeated bit energy E_e is considered to be E_b/N_s due to the fact that one bit is repeated N_s times. Since the chaotic signal, AWGN, and BBNJ are independent of each other and the mean of the AWGN and BBNJ are zero, the mean of the decision variable D_i is the mean of data component U which can be readily expressed as

$$E\left[D_i\right] = E\left[U\right] = \frac{E_e}{2P}, \tag{12}$$

where the repeated bit energy $E_e = 2P\sum_{k=1}^{\beta/P} E\left[x_{i,k}^2\right]$ and $E_e = E_b/N_s$. In addition, the repeated bit energy E_e is assumed to be constant for a high spreading factor β/P. Thus, the variance of the decision variable can be expressed as

$$V\left[D_i\right] = \sum_{u=1}^{5} V\left[N_u\right] + \sum_{v=1}^{3} V\left[I_v\right]. \tag{13}$$

The variance of $\sum_{u=1}^{5} V\left[N_u\right]$, and $\sum_{v=1}^{3} V\left[I_v\right]$ can be obtained as

$$V\left[N_1\right] = \frac{E_e N_0}{2P} = V\left[N_2\right], \tag{14}$$

$$V[N_3] = \frac{\beta N_0 P_j}{2P^3} = V[N_4], \tag{15}$$

$$V[N_5] = \frac{\beta N_0^2}{4P^3}, \tag{16}$$

$$V[I_1] = \frac{E_e P_j}{2P^2} = V[I_2], \tag{17}$$

$$V[I_3] = \frac{\beta P_j^2}{P^3}, \tag{18}$$

where N_0 and P_j is the noise power spectral density and jamming signal power, respectively. By substituting (13) for (14), (15), (16), (17), (18), $V[D_i]$ can be expressed as

$$V[D_i] = \frac{E_b\left(P_j + \frac{N_0}{2}\right)}{P^2} + \beta\frac{\left(P_j + \frac{N_0}{2}\right)^2}{P^3}. \tag{19}$$

For a Gaussian noise and BBNJ environment, the $\widehat{BER}$ for repeated bits can be represented as

$$\widehat{BER} = \frac{1}{2}\Pr(D_l < 0 \,|b_l = +1) + \frac{1}{2}\Pr(D_l > 0 \,|b_l = -1), \tag{20}$$

which can be obtained as

$$\begin{aligned}\widehat{BER} &= \frac{1}{2}erfc\left(\left[\frac{2V[D_i]}{E[D_i]^2}\right]^{-\frac{1}{2}}\right)\\ &= \frac{1}{2}erfc\left(\left[8\frac{\left(P_j + \frac{N_0}{2}\right)}{E_e} + 8\beta\frac{\left(P_j + \frac{N_0}{2}\right)^2}{PE_e^2}\right]^{-\frac{1}{2}}\right)\\ &= \frac{1}{2}erfc\left(\left[8\frac{\left(P_{j_0}/N_sN_h + N_0/2\right)}{E_b/N_s}\right.\right.\\ &\quad \left.\left. + 8\frac{\beta}{P}\frac{\left(P_{j_0}/N_sN_h + N_0/2\right)^2}{\left(E_b/N_s\right)^2}\right]^{-\frac{1}{2}}\right),\end{aligned} \tag{21}$$

where erfc(x) is the complementary error function defined as $erfc(x) \equiv \left(2/\sqrt{\pi}\right)\int_x^\infty \exp\left(-\mu^2\right)d\mu$ and P_{j_0} is the jamming power having the bandwidth before time hopping spreading of the NR-DCSK signal. Under the only AWGN environment, the system BER can also be easily obtained from (21) by fixing $P_{j_0} = P_j = 0$

$$\begin{aligned}\widehat{BER}_{AWGN} &= \frac{1}{2}erfc\left(\left[\frac{4N_0}{E_e} + \frac{2\beta N_0^2}{PE_e^2}\right]^{-\frac{1}{2}}\right)\\ &= \frac{1}{2}erfc\left(\left[4\frac{N_0}{E_b/N_s} + 2\frac{\beta}{P}\frac{N_0^2}{\left(E_b/N_s\right)^2}\right]^{-\frac{1}{2}}\right).\end{aligned} \tag{22}$$

Considering hard decision of N_s repeated bits, the ultimate BER performance of the TH-NRDCSK system can be calculated as

$$BER = \sum_{z=1}^{\lfloor N_s/2\rfloor}\binom{N_s}{N_s - z}\widehat{BER}^{N_s - z}\left(1 - \widehat{BER}\right)^z. \tag{23}$$

Remark : Through the equation (21) and (22), we notice that the jamming power P_j is affected by both N_h and N_s and the repeated bit energy E_e is altered by N_s. Therefore, if the jamming power P_j is much smaller than the noise power spectral density N_0, i.e. $P_j \ll N_0$, we can approximate equation (21) to equation (22). In this case, the BER performance of the TH-NRDCSK system is affected by only N_s. Otherwise, when the jamming power P_j is much bigger than the noise power spectral density N_0, i.e. $P_j \gg N_0$, the BER performance of the TH-NRDCSK system is affected by only N_h.

V. SIMULATION RESULTS

In this section, we simulate the proposed TH-NRDCSK system under six simulation setups to validate the theoretical analysis and observe the effect of system parameters on AJ performance and compare it to conventional counterparts. The BER performance of the TH-NRDCSK system for the parameter P is illustrated in A under the AWGN channel. In addition, B, C, and D shows the AJ performance of the TH-NRDCSK system for several N_h and N_s, under four types of jamming environments, and for several β and P combinations, respectively. Moreover, E and F depicts the AJ performance comparison to conventional counterparts under SJ environment and under time synchronization error condition. The value of simulation parameters for each cases are given in Table 2.

A. BER PERFORMANCE OF THE TH-NRDCSK SYSTEM UNDER AWGN CHANNEL

The analytic and simulated results for the proposed TH-NRDCSK system under the AWGN channel for various P are presented in Fig. 5. This simulation demonstrates that the simulation results entirely validate the analytic BER expression. In addition, the performance is improved as P increases. Specifically, at BER $= 10^{-2}$, the proposed TH-NRDCSK system can obtain about 1dB SJR gain as P is doubled. It is also noteworthy that as P increases, the gap between analysis

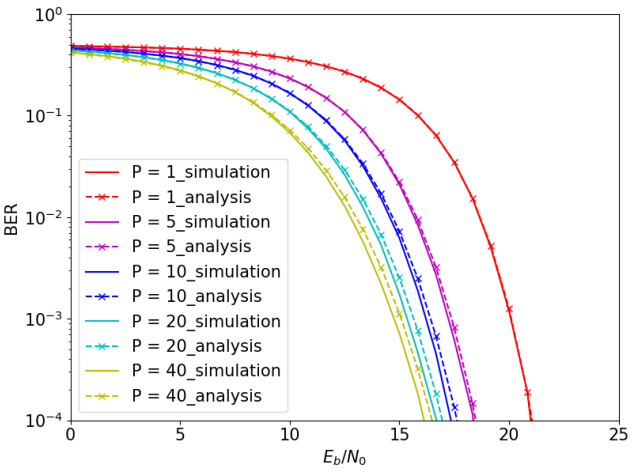

FIGURE 5. BER performance of the TH-NRDCSK system under AWGN channel for various P.

TABLE 2. Simulation value of system parameters.

Parameters	Cases					
	A	B	C	D	E	F
β	200	200	25	$25 \sim 400$	25	25
P	$1 \sim 40$	25	5	Divisor of β	5	5
f_s [Hz]	$2\beta/T_c$					
T_c [s]	1e-09					
N_h	4	2, 4, 6, 8	4	4	4	4
N_s	3	3, 5, 7, 9	3	3	3	3
N_t	100					
Jamming type	x	BBNJ	SJ	SJ	All	SJ
f_l [Hz]	2.5e09					
f_u [Hz]	3.5e09					
E_b/N_0 [dB]	$0 \sim 25$	15	15	15	15	15
SJR [dB]	$-30 \sim 10$	$-30 \sim 10$	$-30 \sim 10$	0	$-30 \sim 10$	$-30 \sim 10$

and simulation curves enlarges. This is because the number of chaotic samples, which can be calculated by β/P, decreases so that the approximation of analysis can not be guaranteed.

B. AJ PERFORMANCE OF THE TH-NRDCSK SYSTEM FOR DIFFERENT N_H AND N_S

Fig. 6 and Fig. 7 present the BER of the proposed TH-NRDCSK system versus SJR with different N_s and N_h values. Since β and P is 200 and 25, respectively in this simulation, the performance gap between analysis and simulation results is identified in Fig. 6 and Fig. 7. Specifically, Fig. 6 illustrates that the AJ performance of the TH-NRDCSK system is degraded as N_s increases due to the fact that the repeated bit energy E_e is decreased by N_s times, i.e. $E_e = E_b/N_s$. Even though the jamming power is lower as N_s increases, the graph in Fig. 6 shows that the AJ performance of the TH-NRDCSK system is degraded. It can be seen that the effect of noise is more effective than the effect of jamming due to the distributed power by N_s.

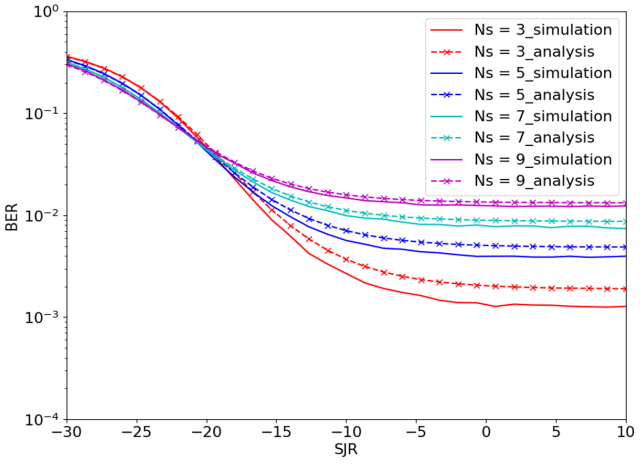

FIGURE 6. AJ performance of the TH-NRDCSK system according to N_s.

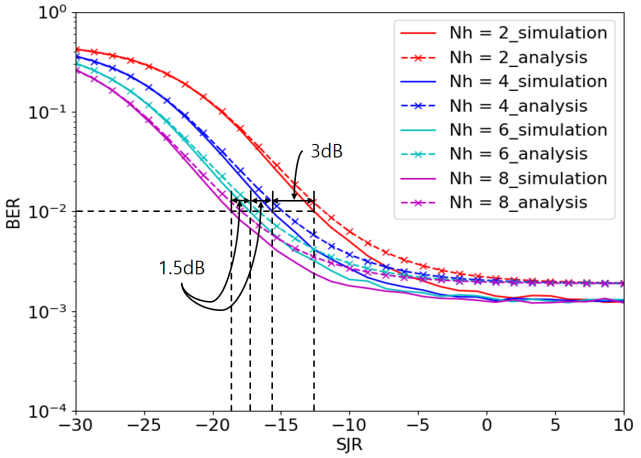

FIGURE 7. AJ performance of the TH-NRDCSK system according to N_h.

Nonetheless, the simulation result gets closer to theoretical analytic results as N_s increases. This is because the weak law of large numbers theory applies as N_s increases. In addition, Fig. 7 shown at the top of next page represents that the AJ performance of the TH-NRDCSK system is improved as N_h increases. Unlike N_s, the larger N_h value gives the more SJR power gain. Particularly, at BER $= 10^{-2}$, the proposed TH-NRDCSK system can obtain about 3dB SJR gain as N_h is doubled. Eventually, the AJ performance of the TH-NRDCSK system is improved as N_s decreases and N_h increases.

C. AJ PERFORMANCE OF THE TH-NRDCSK SYSTEM UNDER DIFFERENT JAMMING TYPE

In Fig. 8, we illustrate the comparison of AJ performance of the TH-NRDCSK system under different jamming types. BBNJ has less impact on the TH-NRDCSK system than other jamming types. Moreover, the TH-NRDCSK system has similar AJ performance against PBNJ and SJ attacks.

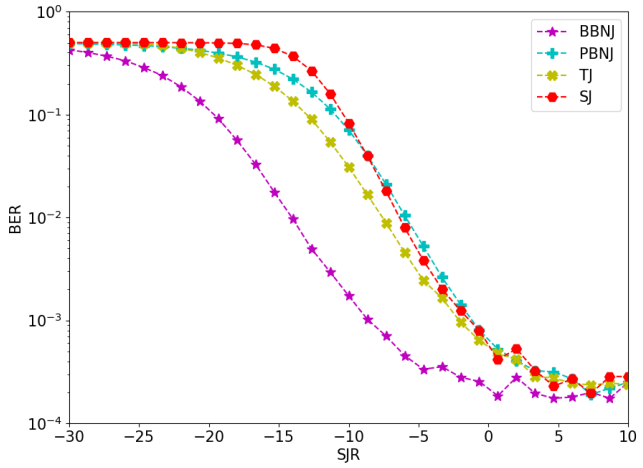

FIGURE 8. AJ performance comparison of the TH-NRDCSK system under four jamming types.

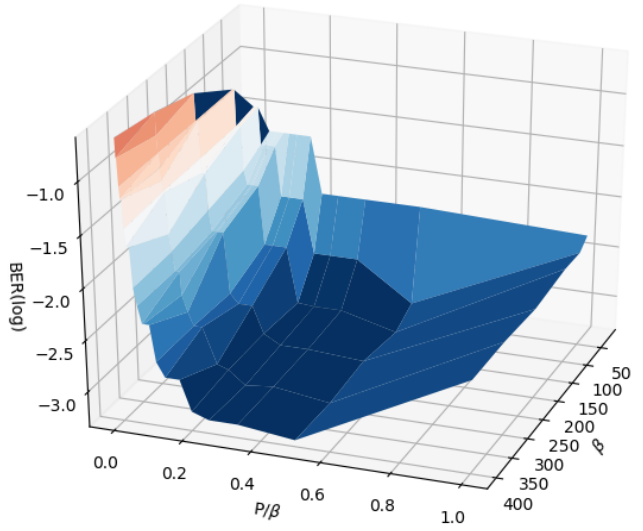

FIGURE 9. AJ performance of the TH-NRDCSK system according to β, P.

However, we notice that SJ has the most powerful effect to the TH-NRDCSK system in low SJR region. As a results, SJ is the most aggressive opponent to TH-NRDCSK system. SJ is also shown to be the most powerful jamming against NR-DCSK system [30]. Beyond the 5dB SJR, however, the effect of all jamming types becomes similar. In subsequent simulations, AJ performance against SJ will continue to be explored.

D. AJ PERFORMANCE OF THE TH-NRDCSK SYSTEM FOR DIFFERENT P AND β

We then simulate the effect of P and β on the AJ performance of the TH-NRDCSK system under the SJ environment. In the simulation, we set β equal to 25, 50, 100, 200, 300, and 400. Correspondingly, P is set to the divisors of β because the number of generated chaotic samples required to present one bit should be β/P.

Fig. 9 shows the BER performance of the proposed system versus P/β. It is shown that the best BER performance is obtained when P/β is 0.5 for any fixed β. When P is equal to β, the AJ performance of the TH-NRDCSK system becomes worse even though P increases. Moreover, Fig. 9 shows that the AJ performance of the TH-NRDCSK system has a similar trend versus P/β for all β, i.e. BER performance is improved until $P/\beta = 0.5$ and degraded at $P/\beta = 1$. One more thing to note is that at $P/\beta = 0.5$, AJ performance is improved as β increases.

E. AJ PERFORMANCE OF THE TH-NRDCSK SYSTEM COMPARED TO CONVENTIONAL SYSTEMS

In Fig. 10, the graph shows a comparison of BER provided by the TH-BPSK, non-coherent TH-BPSK, CSK, NR-DCSK, and proposed TH-NRDCSK systems. It is shown that the coherent TH-BPSK and CSK systems provide a better performance than the non-coherent counterparts. Compared to non-coherent TH-BPSK system at BER $= 10^{-2}$, the proposed TH-NRDCSK system acquires 8.5dB SJR gain. This improvement is definitely achieved by applying the NR-DCSK structure to the non-coherent TH-BPSK system. Moreover, the TH-NRDCSK system exhibits a similar performance to the coherent CSK system below -10dB SJR. Furthermore, the TH-NRDCSK system exhibits a more robust AJ performance than the NR-DCSK system under 8dB SJR. This enhancement is due to the application of THSS system. Eventually, Fig. 10 shows the advantages of integration of two systems definitely.

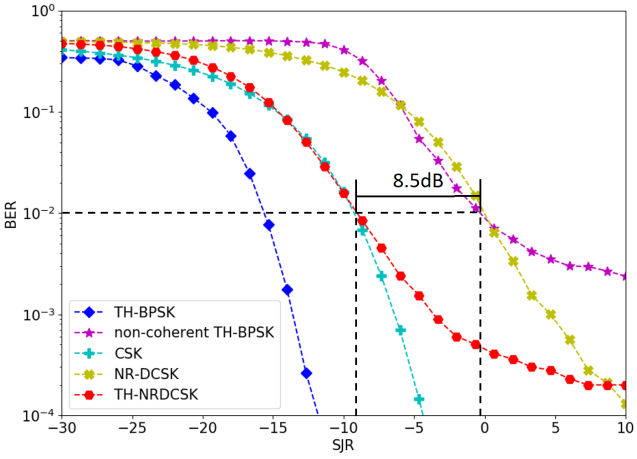

FIGURE 10. AJ performance of the TH-BPSK, non-coherent TH-BPSK, CSK, NR-DCSK, TH-NRDCSK systems.

F. AJ PERFORMANCE OF THE TH-NRDCSK SYSTEM AND COHERENT COUNTERPARTS UNDER THE SYNCHRONIZATION ERROR CONDITION

The AJ performance of the TH-NRDCSK system and coherent counterparts under the time synchronization error condition is shown in Fig. 11. We compare the performance of the TH-NRDCSK system with that of the TH-BPSK

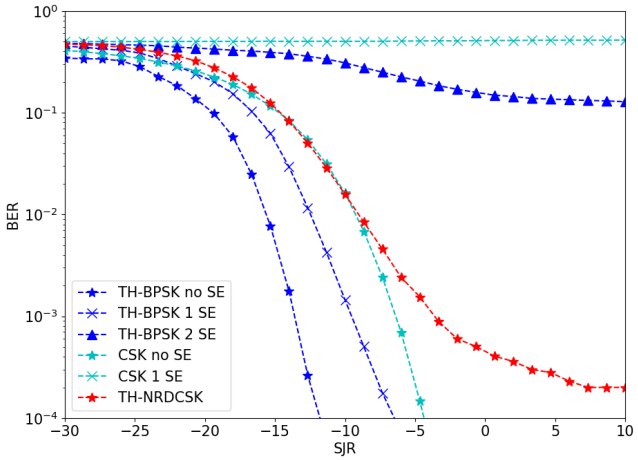

FIGURE 11. AJ performance comparison of the coherent system (TH-BPSK, CSK) and TH-NRDCSK system under synchronization error (SE) condition.

and CSK system by simulating under no, 1, and 2 samples synchronization error conditions. 1 and 2 sample synchronization error means 1 and 2 sample time mismatch of the mask signal and the received signal in the coherent system so that it makes the information bits not restored properly. On the other hand, the non-coherent system that does not use a mask signal does not need to care about time synchronization error. In the Fig. 11, the performance of the non-coherent TH-NRDCSK system is inherently worse than that of the coherent TH-BPSK and CSK systems under no synchronization error. However, when the synchronization error occurs, the performance of the coherent system is drastically degraded. When 2 samples error occurs, both coherent TH-BPSK and CSK systems would be ineffective. On the other hand, the BER performance of the TH-NRDCSK system is barely affected by synchronization error. This simulation illustrates the reason why the non-coherent system is more preferable in reality.

VI. CONCLUSION

In this paper, we first proposed a hybrid TH-NRDCSK system to enhance the BER performance of the conventional non-coherent THSS system against jamming attacks. The TH-NRDCSK system is a THSS system that utilizes NR-DCSK signal instead of conventional THSS pulses.

Secondly, we analytically derived the BER expression of the proposed system under a AWGN channel and under BBNJ environment and verified the derived BER performance by simulation results. The BER performance versus E_b/N_0 is improved by increasing P. In addition, the AJ performance of the TH-NRDCSK system is improved as N_s decreases and N_h increases independently.

Other simulations are provided to observe the AJ performance of the TH-NRDCSK system under several simulation setups. We present that SJ is shown to be the most powerful among the four jamming types to the TH-NRDCSK system which is the reason why SJ is used in subsequent simulations. Moreover, the case when P is half of β has the best performance for any fixed β. We also demonstrate that the time synchronization problem has a serious impact on coherent systems. Finally, we showed that the TH-NRDCSK outperforms other non-coherent counterparts.

REFERENCES

[1] A. T. Elsworth, *Electronic Warfare*. New York, NY, USA: Nova, 2010.
[2] Y. Zou, J. Zhu, X. Wang, and L. Hanzo, "A survey on wireless security: Technical challenges, recent advances, and future trends," *Proc. IEEE*, vol. 104, no. 9, pp. 1727–1765, Sep. 2016.
[3] J. Omura, R. Scholtz, and B. Levitt, *Spread Spectrum Communications Handbook, Electronic Edition*. New York, NY, USA: McGraw-Hill, 2002.
[4] M. Z. Win and R. A. Scholtz, "Ultra-wide bandwidth time-hopping spread-spectrum impulse radio for wireless multiple-access communications," *IEEE Trans. Commun.*, vol. 48, no. 4, pp. 679–689, Apr. 2000.
[5] Z. Bai, S. Peng, Q. Zhang, and N. Zhang, "OCC-selection-based high-efficient UWB spatial modulation system over a multipath fading channel," *IEEE Syst. J.*, vol. 13, no. 2, pp. 1181–1189, Jun. 2018.
[6] B. Hu and N. C. Beaulieu, "Accurate evaluation of multiple-access performance in TH-PPM and TH-BPSK UWB systems," *IEEE Trans. Commun.*, vol. 52, no. 10, pp. 1758–1766, Oct. 2004.
[7] Z. Sahinoglu, I. Guvenc, P. Orlik, and A. F. Molisch, "Interference suppression in non-coherent time-hopping IR-UWB ranging," in *Proc. IEEE Int. Conf. Ultra-Wideband*, Sep. 2006, pp. 507–511.
[8] W.-D. Chang, S.-P. Shih, and C.-Y. Chen, "Chaotic secure communication systems with an adaptive state observer," *J. Control Sci. Eng.*, vol. 2015, Jan. 2015, Art. no. 15.
[9] C. Hua, B. Yang, G. Ouyang, and X. Guan, "A new chaotic secure communication scheme," *Phys. Lett. A*, vol. 342, no. 4, pp. 305–308, 2005.
[10] B. Jovic, C. P. Unsworth, G. S. Sandhu, and S. M. Berber, "A robust sequence synchronization unit for multi-user DS-CDMA chaos-based communication systems," *Signal Process.*, vol. 87, no. 7, pp. 1692–1708, 2007.
[11] X. Yang, Z. Yang, and X. Nie, "Exponential synchronization of discontinuous chaotic systems via delayed impulsive control and its application to secure communication," *Commun. Nonlinear Sci. Numer. Simul.*, vol. 19, no. 5, pp. 1529–1543, 2014.
[12] M. Zapateiro, Y. Vidal, and L. Acho, "A secure communication scheme based on chaotic Duffing oscillators and frequency estimation for the transmission of binary-coded messages," *Commun. Nonlinear Sci. Numer. Simul.*, vol. 19, no. 4, pp. 991–1003, Apr. 2014.
[13] H. A. Abdullah and H. N. Abdullah, "A new chaotic map for secure transmission," *Telecommun. Comput. Electron. Control (TELKOMNIKA)*, vol. 16, no. 3, pp. 1135–1142, 2018.
[14] M. F. Hassan and M. Hammuda, "A new approach for constrained chaos synchronization with application to secure data communication," *J. Franklin Inst.*, vol. 356, no. 12, pp. 6697–6723, 2019.
[15] D.-P. Vuong, D.-K. Le, K.-K. Nguyen, and B. Van Nguyen, "Correlation receiver with nonlinearity blanking for DCSK systems under pulse jamming attack," *IEEE Access*, vol. 7, pp. 25037–25045, 2019.
[16] B. Van Nguyen, M. T. Nguyen, H. Jung, and K. Kim, "Designing anti-jamming receivers for NR-DCSK systems utilizing ICA, WPD, and VMD methods," *IEEE Trans. Circuits Syst., II, Exp. Briefs*, vol. 66, no. 9, pp. 1522–1526, Sep. 2019.
[17] A. Tayebi, S. Berber, and A. Swain, "Security enhancement of fix chaotic-DSSS in WSNs," *IEEE Commun. Lett.*, vol. 22, no. 4, pp. 816–819, Apr. 2018.
[18] G. Kaddoum, "Wireless chaos-based communication systems: A comprehensive survey," *IEEE Access*, vol. 4, pp. 2621–2648, 2016.
[19] F. C. M. Lau, M. Ye, C. K. Tse, and S. F. Hau, "Anti-jamming performance of chaotic digital communication systems," *IEEE Trans. Circuits Syst. I, Fundam. Theory Appl.*, vol. 49, no. 10, pp. 1486–1494, Oct. 2002.
[20] H. Yang and G.-P. Jiang, "High-efficiency differential-chaos-shift-keying scheme for chaos-based noncoherent communication," *IEEE Trans. Circuits Syst., II, Exp. Briefs*, vol. 59, no. 5, pp. 312–316, May 2012.
[21] G. Kaddoum, E. Soujeri, C. Arcila, and K. Eshteiwi, "I-DCSK: An improved noncoherent communication system architecture," *IEEE Trans. Circuits Syst., II, Exp. Briefs*, vol. 62, no. 9, pp. 901–905, Sep. 2015.

[22] G. Kaddoum, E. Soujeri, and Y. Nijsure, "Design of a short reference non-coherent chaos-based communication systems," *IEEE Trans. Commun.*, vol. 64, no. 2, pp. 680–689, Jan. 2016.
[23] H. Yang and G.-P. Jiang, "Reference-modulated DCSK: A novel chaotic communication scheme," *IEEE Trans. Circuits Syst., II, Exp. Briefs*, vol. 60, no. 4, pp. 232–236, Apr. 2013.
[24] G. Kaddoum and E. Soujeri, "NR-DCSK: A noise reduction differential chaos shift keying system," *IEEE Trans. Circuits Syst., II, Exp. Briefs*, vol. 63, no. 7, pp. 648–652, Jul. 2016.
[25] G. Boeing, "Visual analysis of nonlinear dynamical systems: Chaos, fractals, self-similarity and the limits of prediction," *Systems*, vol. 4, no. 37, p. 37, Nov. 2016.
[26] R. A. Poisel, *Modern Communications Jamming Principles and Techniques*, 2nd ed. Norwood, MA, USA: Artech House, 2011.
[27] A. E. Mansour, W. M. Saad, and S. H. El Ramly, "Cross-coupled chaotic matched frequency hopping in presence of partial band noise jamming," in *Proc. 11th Int. Conf. Comput. Eng. Syst. (ICCES)*, Dec. 2016, pp. 355–359.
[28] G. Mazurek, "Jamming protection of spread spectrum RFID system," *Proc. SPIE*, vol. 6347, Oct. 2006, Art. no. 634721.
[29] M. G. Amin, "Interference mitigation in spread spectrum communication systems using time-frequency distributions," *IEEE Trans. Signal Process.*, vol. 45, no. 1, pp. 90–101, Jan. 1997.
[30] B. Van Nguyen, H. Jung, and K. Kim, "On the antijamming performance of the NR-DCSK system," *Secur. Commun. Netw.*, vol. 2018, pp. 1–8, Feb. 2018.

JUNGMIN KIM (M'18) received the B.S. degree in electronic engineering from Pusan National University (PNU), Busan, South Korea, in 2018. He is currently pursuing the M.S. degree in electrical and electronic computer engineering with the Gwangju Institute of Science and Technology (GIST), Gwangju, South Korea. His research interests include time hopping, and chaotic and anti-jamming communication systems.

BINH VAN NGUYEN received the bachelor's degree in electrical and electronics from the Ho Chi Minh City University of Technology, Ho Chi Minh City, Vietnam, in 2010, and the M.S. and Ph.D. degrees in wireless communications from the Gwangju Institute of Science and Technology (GIST), Gwangju, South Korea, in 2012 and 2016, respectively, where he was a Research Fellow, from September 2016 to October 2018, and an Assistant Research Professor, from November 2018 to August 2019. He is currently with Samsung Electronics, Suwon, South Korea, and with the Institute of Research and Development, Duy Tan University, Da Nang, Vietnam. His research interests include cooperative communications, physical layer security, and chaotic and anti-jamming communications.

HYOYOUNG JUNG received the B.S. degree from Inha University, in 2011, and the M.S. degree from the Gwangju Institute of Science and Technology (GIST), South Korea, in 2013, where he is currently pursuing the Ph.D. degree. His research interests include information theory, estimation theory, and time-hopping and anti-jamming communication systems.

KISEON KIM received the B.Eng. and M.Eng. degrees in electronics engineering from Seoul National University, Seoul, South Korea, in 1978 and 1980, respectively, and the Ph.D. degree in electrical engineering systems from the University of Southern California at Los Angeles, Los Angeles, CA, USA, in 1987. From 1988 to 1991, he was with Schlumberger, Houston, TX, USA. From 1991 to 1994, he was with the Superconducting Super Collider Laboratory, Waxahachie, TX, USA. In 1994, he joined the Gwangju Institute of Science and Technology, Gwangju, South Korea, where he is currently a Professor. His current research interests include wideband digital communications system design, sensor network design, analysis and implementation both at the physical and at the resource management layer, and biomedical application design. He is also a member of the National Academy of Engineering of Korea, a Fellow of the IET, and a Senior Editor of the IEEE SENSORS JOURNAL.